



1 **Contribution of the Sensitivity Analysis in Groundwater Vulnerability Assessing Using the**

2 **DRASTIC and Composite DRASTIC Indexes**

3 Mohammad Malakootian<sup>1</sup>, Majid Nozari,<sup>\*</sup>

4 **Manuscript Authors details:**

5 1. Mohammad Malakootian, Department of Environmental Health, School of Public Health,

6 Kerman University of Medical Sciences, Iran. E-mail: m.malakootian@yahoo.com.

7 <https://orcid.org/0000-0002-4051-6242>.

8 2. Majid Nozari, Department of Environmental Health, School of Public Health, Kerman

9 University of Medical Sciences, Iran. Tel: 98-9383921819, E-mail: nozari.m@kmu.ac.ir.

10 <https://orcid.org/0000-0003-2319-1930>.

11

12

13

14

15

16

17

18

19

20

21

22



23 **ABSTRACT**

24 The present study estimates Kerman–Baghin aquifer vulnerability by applying the DRASTIC  
25 and composite DRASTIC (CDRASTIC) indexes. The factors affecting the transfer of  
26 contamination, including the water table depth, soil media, aquifer media, the impact of the  
27 vadose zone, topography, hydraulic conductivity, and land use, were ranked, weighted, and  
28 integrated using a geographical information system (GIS). A sensitivity test has also been  
29 performed to specify the sensitivity of the parameters. The study results show that the  
30 topographic layer displays a gentle slope in the aquifer. The majority of the aquifer covered  
31 irrigated field crops and grassland with a moderate vegetation cover. In addition, the aquifer  
32 vulnerability maps indicate very similar results, recognizing the northwest parts of the aquifer as  
33 areas with high and very high vulnerability. The map removal sensibility analysis (MRSA)  
34 revealed the impact of the vadose zone (in the DRASTIC index) and hydraulic conductivity (in  
35 the CDRASTIC index) as the most effective parameters in the vulnerability evaluation. In both  
36 indexes, the single-parameter sensibility analysis (SPSA) showed net recharge as the most  
37 effective factor in the vulnerability estimation. From this study, it can be concluded that  
38 vulnerability maps can be used as a tool to control human activities for the sustained protection  
39 of aquifers.

40

41 **Keywords:** Vulnerability; Sensitivity analyses; DRASTIC; Composite DRASTIC; Kerman–  
42 Baghin aquifer

43

44

45

46



47 **1. Introduction**

48 Groundwater's are as a significant and principal resource in most parts of the world, especially  
49 for those in waterless and arid areas. Water quality has been given more affirm on groundwater's  
50 control (Neshat et al., 2014;Manap et al., 2013;Manap et al., 2014a;Ayazi et al., 2010). The  
51 potential groundwater's contamination by mankind operations at or near the surface of the  
52 groundwater has been supposed the major base for control of this source (Tilahun and Merkel,  
53 2010).

54 The introduction of potential contaminants to a location on top of an aquifer at a specified  
55 position in an underground system is defined as groundwater vulnerability (Sarah and Patricia I,  
56 1993;Neshat et al., 2014). Groundwater vulnerability is an estimate of the relative hazard of  
57 groundwater pollution by a specific constituent. Vulnerability maps are commonly performed at  
58 a sub-basin, basin, or regional scale. They are not normally applied for site-specific estimates  
59 including zones smaller than a few tens of square kilometers (Baalousha, 2006;Tilahun and  
60 Merkel, 2010). Different techniques have been presented to assess groundwater susceptibility  
61 with great precision (Javadi et al., 2010;Javadi et al., 2011). Mostly, these methods including  
62 analytic tools considered to relate groundwater contamination with land operations. There are  
63 three types of evaluation methods include; the overlay and index, the process-based simulation  
64 and, the statistic procedures (Neshat et al., 2014;Dixon, 2004).

65 Overlay and index procedures affirm the incorporation of various zonal maps by allocating  
66 a numeral index. Both procedures are simple to use in the geographic information system,  
67 especially on a zonal measure. Hence, these methods are the most famous procedures applied to  
68 vulnerability estimation (Neshat et al., 2014). The most extensively utilized among these  
69 methods encompass GODS (Ghazavi and Ebrahimi, 2015), IRISH (Daly and Drew, 1999), AVI



70 (Raju et al., 2014), and DRASTIC (Neshat et al., 2014;Baghapour et al., 2014;Baghapour et al.,  
71 2016).

72 The DRASTIC index for the first time proposed by Aller et al (1985). It is considered one of  
73 the best indexes for the vulnerability of groundwater. This method ignores the influences of  
74 zonal properties. Thus, identical weights and rating values are utilized. In addition, this technique  
75 does not apply a standard validation test for the aquifer. Therefore, several investigators  
76 developed this index using various techniques (Neshat et al., 2014). The higher DRASTIC index  
77 represents the greater contamination potential and inversely. After calculating, the DRASTIC  
78 index should be possible to identify the zones that are more prone to pollution. This index only  
79 provides a relative estimate and is not created to make a complete assessment (Baalousha, 2006).

80 Many studies have been conducted using DRASTIC index to estimate the groundwater  
81 vulnerability in the world different regions (Jaseela et al., 2016;Zghibi et al., 2016;Kardan  
82 Moghaddam et al., 2017;Kumar et al., 2016;Neshat and Pradhan, 2017;Souleymane and Tang,  
83 2017;Ghosh and Kanchan, 2016;Saida et al., 2017), however, fewer studies have used the  
84 CDRASTIC index for evaluation of the groundwater vulnerability (Baghapour et al.,  
85 2016;Baghapour et al., 2014;Secunda et al., 1998;Jayasekera et al., 2011;Shirazi et al.,  
86 2012;Jayasekera et al., 2008). Boughriba et al. (2010) utilized DRASTIC index in geographical  
87 information system environment for an estimate of the vulnerability in the aquifer. They provide  
88 the DRASTIC modified map prepared from total DRASTIC indexes and small monitoring  
89 network maps inclusive two classes, high and medium. Then they integrated the map with the  
90 land use map to provide the contamination potential map. They reported that the new obtained  
91 map inclusive three various classes very high, medium, and high. Babiker et al. (2005) used the  
92 DRASTIC index to determine prone points to contamination from human activities in the



93 aquifer. They reported that the western and eastern parts of aquifer fall in the high and medium  
94 categories, respectively. The final aquifer vulnerability map represents that the high risk of  
95 pollution is in the eastern part of aquifer due to agriculture activities. They also observed that the  
96 factor, net recharge has the most effect on the aquifer vulnerability, followed by the soil media,  
97 topography, the impact of the vadose zone, and hydraulic conductivity.

98 The water difficulties in Iran with a mean annual rainfall about one-third of the world annual  
99 rainfall (Chitsazan and Akhtari, 2006; Modabberi et al., 2017) are critical and serious. Also,  
100 diminution in these rare resources has deteriorated this condition. Groundwater is the only water  
101 source in the Kerman province due to the lack of surface water. The evaluated aquifer in this  
102 research located in the central part of Kerman province in Iran. Due to recent droughts, this  
103 aquifer is placed under heavy pumping to irrigate crops, which cause gradually reduces the water  
104 level. Moreover, recently, the use of groundwater resources has been greater than in former  
105 years. It causes the researches on the pathology and zoning the losses in groundwater undeniable.  
106 Therefore, the purpose of this research is providing the Kerman–Baghin aquifer vulnerability  
107 maps and performing the sensitivity analysis to identify the most effective factors in the  
108 vulnerability.

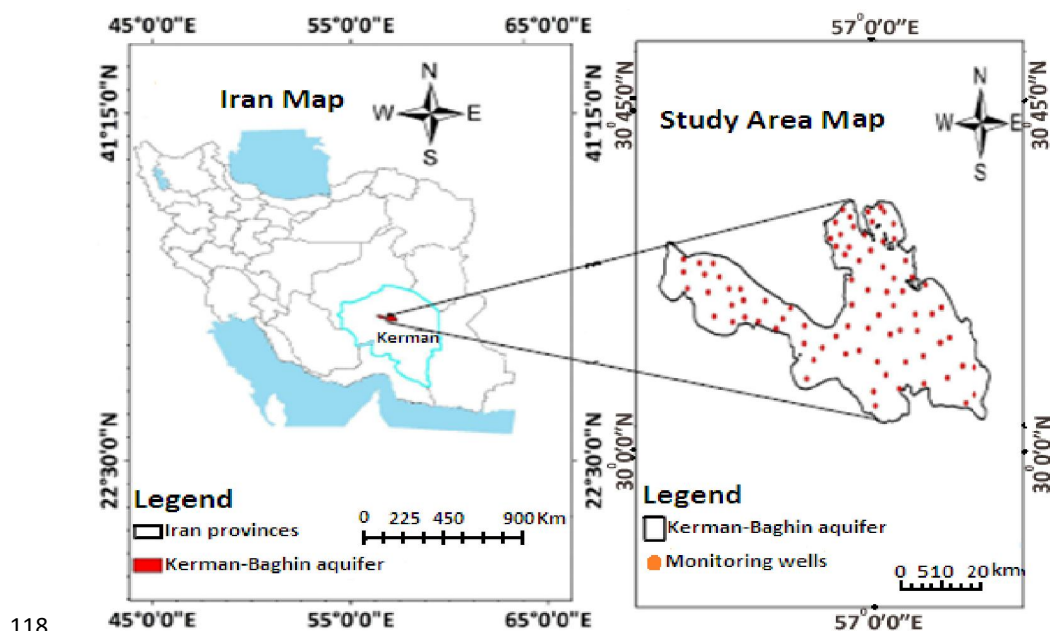
## 109 **2. Methodology**

### 110 **2.1. Study area**

111 The Kerman Province covers both semiarid and waterless areas. The present study included a  
112 2023 km<sup>2</sup> area (29° 47' to 30° 31' N latitude and 56° 18' to 57° 37' E longitude) located in the  
113 central part of the Kerman Province, Iran (Figure 1). The study area is mostly covered by  
114 agricultural land (Neshat et al., 2014). The mean annual rainfall in the study area is 108.3 mm (in  
115 2017). The highest and lowest ground elevation in the study area is 1,980 and 1,633 m above sea



116 level, respectively. The mean, minimum, and maximum annual temperatures in the study area  
117 are 17°C, -12°C, and 41°C, respectively (in 2017).



118  
119 **Fig. 1.** Location map of the Kerman–Baghin aquifer

## 120 **2.2. Computing the DRASTIC and CDRASTIC indexes**

121 DRASTIC is a procedure developed by the United States Environmental Protection Agency (U.S  
122 EPA) to prepare a systematic estimate of the potential for groundwater pollution (Aller et al.,  
123 1985). Through this method, the DRASTIC index is obtained from the sum of the multiplication  
124 of the rank and weight of the parameters. Higher sum values demonstrate greater vulnerability of  
125 the aquifer to pollution. Vulnerability ranges corresponding to the DRASTIC index are presented  
126 in Table 1. In the DRASTIC index, each parameter is rated on a scale from 1 to 10 that shows the  
127 relative contamination potential of that parameter for that area. Also, in the DRASTIC index, one  
128 weight is assigned to each of the parameters (1 to 5). Weight values show the relative



129 significance of the parameters with respect to each other. The DRASTIC index is obtained using  
 130 the following formula (Kardan Moghaddam et al., 2017; Neshat and Pradhan, 2017):

131 
$$\text{DRASTIC index} = D_r D_w + R_r R_w + A_r A_w + S_r S_w + T_r T_w + I_r I_w + C_r C_w. \quad (1)$$

132 In the above formula, the letters in the acronym DRASTIC comprise a short form of the effective  
 133 factors in the DRASTIC index. Also, “r” and “w” are the rating and weight of each factor,  
 134 respectively. The ratings and weights of the factors are depicted in Table 2.

135 **Table 1** The range of vulnerability related to the DRASTIC index

Vulnerability	Ranges
Very low	23-46
Low	47-92
Moderate	93-136
High	137-184
Very high	>185

136

137 **Table 2** Rating and weight related to DRASTIC index factors

DRASTIC parameters	Range	Rating (r)	Weight (w)
Water table depth (m)	0.0-1.5	10	5
	1.5-4.6	9	
	4.6-9.1	7	
	9.1-15.2	5	
	15.2-22.9	3	
	22.9-30.5	2	
	>30.5	1	
Aquifer media	Rubble and sand	9	3
	Gravel and sand	7	
	Gravel, sand, clay and silt	5	
	Sand and clay	4	
	Sand, clay and silt	3	
Soil media	Rubble, sand, clay and silt	9	2
	Gravel and sand	7	
	Gravel, sand, clay and silt	6	
	Sand	5	
	Sand, clay and silt	3	
	clay and silt	2	



Topography or slope (%)	0-2	10	
	2-6	9	
	6-12	5	1
	12-18	3	
	>18	1	
The impact of the vadose zone	Rubble, sand, clay and silt	9	
	Gravel and sand	7	
	Gravel, sand, clay and silt	5	5
	Sand, clay and silt	3	
Hydraulic conductivity (m/day)	0-4.1	1	
	4.1-12.2	2	3
	12.2-28.5	4	
	28.5-40.7	6	
	40.7-81.5	8	

138

139 To get the CDRASTIC index, an additional factor (land use) is added to the above formula.

140 Thus, the CDRASTIC index was obtained as follows:

$$141 \quad \text{CDRASTIC index} = D_r D_w + R_r R_w + A_r A_w + S_r S_w + T_r T_w + I_r I_w + C_r C_w + L_r L_w. \quad (2)$$

142 In the above formula,  $L_w$  and  $L_r$  are the relative weight and rating related to the land use factor,  
 143 respectively. Ratings and weightings applied to the pollution potential, which are related to the land  
 144 use factor based on the CDRASTIC index, are indicated in Table 3. The output of the CDRASTIC  
 145 index should be within the range of 28 to 280. Vulnerability ranges based on the CDRASTIC index  
 146 are presented in Table 4.

147 **Table 3** Ratings and weighting applied to the pollution potential related to the land use factor  
 148 based on the CDRASTIC index

	Land use	Rating	Weight
Irrigated field crops + Urban areas		10	
Irrigated field crops + Grassland with poor vegetation cover + Urban areas		9	
Irrigated field crops + Grassland with moderate vegetation cover + Urban areas		8	
Irrigated field crops		8	
Irrigated field crops + Fallow land + Grassland with poor vegetation cover		7	
Irrigated field crops + Grassland with poor vegetation cover		7	
Irrigated field crops + Grassland with moderate vegetation cover		6	
Irrigated field crops + Rocky + Urban areas		5	5





Irrigated field crops + Grassland with poor vegetation cover + Woodland	5
Irrigated field crops + Woodland	5
Irrigated field crops + Rocky	4
Fallow land	3
Fallow land + Grassland with poor vegetation cover	3
Fallow land + Grassland with moderate vegetation cover	3
Grassland with poor vegetation cover	2
Grassland with moderate vegetation cover	2
Grassland with moderate vegetation cover + Woodland	1
Sand dune + Grassland with moderate vegetation cover	1
Sand dune	1

149

150 **Table 4** Vulnerability ranges related to the CDRASTIC index

Vulnerability	Ranges
Very low	<100
Low	100-145
Moderate	145-190
High	190-235
Very high	≥235

151 **2.3. Water table depth**

152 The water table depth factor is the depth from the Earth’s surface to the water table in a well  
 153 (Baghapour et al., 2016). To obtain this factor from existing information, 83 wells in the  
 154 Kerman–Baghin aquifer were utilized. The interpolation procedure was used to provide a raster  
 155 map of the water table depth factor, which was categorized based on Table 2.

156 **2.4. Net recharge**

157 Net recharge is the amount of runoff that permeates to the Earth and reaches the groundwater  
 158 surface (Singh et al., 2015; Ghosh and Kanchan, 2016). This research uses the Piscopo method  
 159 (Chitsazan and Akhtari, 2009) to provide the net recharge layer for the Kerman–Baghin aquifer  
 160 according to the following equation and Table 5:

161 Net recharge factor = slope (%) + rainfall + soil permeability. (3)



162 In the above equation, the percentage of slope was calculated from a digital elevation model,  
 163 which was obtained from a topographical map. Also, a soil permeability map was created using  
 164 the Kerman–Baghin aquifer soil map (with scale 1:250000) and the drilling logs of the wells  
 165 (number of wells: 83). In the end, a map of the area’s rainfall rate was compiled based on the  
 166 annual average precipitation. Ratings and weights of the net recharge factor are illustrated in  
 167 Table 5.

168 **Table 5** Weight, rating, and range of the net recharge parameter

Slope (%)		Rainfall		Soil permeability		Net Recharge		
Range (%)	Factor	Range (mm/year)	Factor	Range	Factor	Range (cm/year)	Rating	Weight
<2	4	>850	4	High	5	11-13	10	4
2-10	3	700-850	3	Moderate to high	4	9-11	8	
10-33	2	500-700	2	Moderate	3	7-9	5	
>33	1	<500	1	Low	2	5-7	3	
				Very low	1	3-5	1	

169 **2.5. Aquifer media**

170 This parameter controls the path of groundwater streams in the aquifer (Aller et al., 1985;Singh  
 171 et al., 2015). To obtain this layer, the well’s drilling log data (number of wells: 83) in the aquifer  
 172 were used. The data were gathered from the Kerman Regional Water Office (KRWO). The range  
 173 of the aquifer media layer is shown in Table 2.

174 **2.6. Soil media**

175 The soil media has a considerable effect on the amount of water surface that can penetrate into  
 176 the aquifer. Therefore, where the soil layer is thick, the debilitation processes such as absorption,  
 177 filtration, degradation, and evaporation may be considerable (Singh et al., 2015). A soil media  
 178 raster map was provided using the Kerman–Baghin aquifer soil map and the well’s drilling logs.



179 **2.7. Topography**

180 The topography controls the duration of water remaining on the soil surface and the degree of  
181 penetration (Singh et al., 2015). For obtain this layer, the percentage of the slope was provided  
182 from a digital elevation model, which was obtained from the topographical map. The data were  
183 gathered from the KRWO. The range of the topographic layer is presented in Table 2.

184 **2.8. The impact of the vadose zone**

185 The vadose zone is outlined as the area above the groundwater level which is unsaturated (Singh  
186 et al., 2015). This layer plays a considerable role in decreasing groundwater contamination by  
187 pollutant debilitation processes such as purification, chemical reaction, and dispersal (Shirazi et  
188 al., 2012). In order to prepare this layer, from the wells drilling log data (number of wells: 83) in  
189 the aquifer were used. The data were gathered from the KRWO. The range of the impact of the  
190 vadose zone layer is depicted in Table 2.

191 **2.9. Hydraulic conductivity**

192 The hydraulic conductivity refers to the capability of aquifer matters to transfer water. The high  
193 hydraulic conductivity areas demonstrate a high potential for groundwater contamination (Singh  
194 et al., 2015; Aller et al., 1985). To prepare this layer, pumping tests of wells were used (number  
195 of wells: 83). The range of the hydraulic conductivity layer is shown in Table 2.

196 **2.10. Land use**

197 Groundwater is drastically connected with the perspective and land use that it underlies. Land  
198 use influences groundwater resources via variation in recharge and by changing demands for  
199 water. Land use is obligatory since it is required by the CDRASTIC index. The Indian remote



200 sensing satellite information was utilized to providing land use raster map. The weight and rating  
201 related to the land use layer are presented in Table 3.

## 202 **2.11. Sensitivity Analyses**

203 One of the main advantages of the DRASTIC index is the performance of evaluation using a  
204 more number of input data which can restrict the effects of errors or mistakes on the final results.  
205 Nevertheless, some investigators, like Babiker et al. (2005), Barber et al. (1993), and Merchant  
206 (1994), reported that we could obtain similar results using fewer data and lower costs. The  
207 unavoidable subjectivity related to the choice of the seven factors, ranks, and weights utilized to  
208 calculate the vulnerability index has also been criticized. Therefore, in order to eliminate the  
209 aforementioned criticisms, two sensitivity analyses were performed as follows (Napolitano and  
210 Fabbri, 1996):

### 211 **A. MRSA**

212 MRSA value indicates the sensibility of the vulnerability map to eliminating one or more maps  
213 from the suitability analysis. MRSA is calculated as follows (Babiker et al., 2005; Martínez-  
214 Bastida et al., 2010; Saidi et al., 2011; Modabberi et al., 2017):

$$215 \quad S = \left[ \left| \frac{\frac{V}{N} - \frac{V'}{n}}{V} \right| \right] \times 100 \quad (4)$$

216 In this formula, S is the sensibility value expressed in terms of variation index. V is the intrinsic  
217 vulnerability index (real vulnerability index) index and V' is the intrinsic vulnerability index  
218 after removal of factor X. N and n are the numbers of data factors utilized to calculate V and V',  
219 respectively (Babiker et al., 2005; Martínez-Bastida et al., 2010; Saidi et al., 2011; Modabberi et  
220 al., 2017).



## 221 B. SPSA

222 SPSA was presented by Napolitano and Fabbri (1996) for the first time. This test shows the  
223 effect of each of the DRASTIC factors in the final vulnerability index. Using this test derived  
224 from equation 5, the real and effective weight of each factor compared to the theoretical weight  
225 assigned by the analytical model (Babiker et al., 2005;Martínez-Bastida et al., 2010;Saidi et al.,  
226 2011;Modabberi et al., 2017).

$$227 \quad W = \left[ \frac{P_r P_w}{V} \right] \times 100 \quad (5)$$

228 In this above equation,  $W$  is the effective weight of each factor.  $P_r$  and  $P_w$  are the rank and  
229 weight assigned to factor  $P$ , respectively.  $V$  is the intrinsic vulnerability index (Martínez-Bastida  
230 et al., 2010;Babiker et al., 2005;Saidi et al., 2011;Modabberi et al., 2017).

## 231 3. Results and discussion

### 232 3.1. DRASTIC and CDRASTIC parameters

233 Based on the data shown in Table 2, the assigned rating of water table depth varies from 1 to 10.  
234 In addition, based on the results presented in Table 6, the water table depth in the aquifer varies  
235 from 4.6 to >30.5 m (rating 1 to 7). Around 27.55% of the aquifer has a depth of >30.5 m, and  
236 66.16 % of the aquifer has a depth between 9.1 m and 30.5 m. Less than 7% has a depth between  
237 4.6 m and 9.1 m. The Kerman–Baghin aquifer rated map of water table depth factor is presented  
238 in Figure 2(A). According to Figure 2(A) and Table 6, the least impact of the water table depth  
239 parameter on aquifer vulnerability occurs in parts of the center (6.39%), whereas the water table  
240 depth parameter most influences vulnerability in parts of the north, south, northwest, and  
241 southeast (27.55%).



242 According to the results presented in Table 6, 75.81% of the aquifer has a net recharge value  
243 in the range of 7 to 9 cm/year. The highest rating of 8 is dedicated only to 11.74% of the aquifer  
244 that has a net recharge value between 9 and 11 cm/year. The Kerman–Baghin aquifer rated map  
245 of the net recharge parameter is shown in Figure 2(B). According to Piscopo's method, the  
246 Kerman–Baghin aquifer was divided into three classes with regards to the net recharge factor.  
247 The highest net recharge value was seen in the north, northeast, south, southwest, parts of the  
248 northwest, parts of the center, and parts of the southeast (75.81%), whereas the least net recharge  
249 value appeared in parts of the northwest and center (11.74%), as shown in Figure 2(B) and Table  
250 6.

251 As observed in Table 6, the majority of the Kerman–Baghin aquifer media is composed of  
252 sand, clay, and silt (75.21%). The Kerman–Baghin aquifer rated map of aquifer media is  
253 presented in Figure 3(A). Parts of the aquifer in the north, northwest, northeast, center, and  
254 southeast are composed of sand, clay, and silt. Parts of the aquifer in the northwest are composed  
255 of rubble and sand (5.58%). Parts of the aquifer in the south and northwest are composed of  
256 gravel and sand (8.95%), and gravel, sand, clay, and silt (10.26%).

257 The Kerman–Baghin aquifer rated map of the soil media parameter is presented in Figure  
258 3(B). The soil map depicts six different classes of the soil. The highest rank (rank = 9) was  
259 assigned to rubble, sand, clay, and silt (a combination of rubble, sand, clay and silt soils). Also,  
260 the lowest rank (rank = 2) was assigned to clay and silt (a combination of clay and silt soils).  
261 Most of the aquifer soil media is covered with silt, sand, and clay (about 80%).

262 The Kerman–Baghin aquifer rated map of the topography parameter is indicated in Figure  
263 4(A). The topographical layer shows a gentle slope (0 to 6%) over most of the aquifer, hence  
264 gaining ranks of 9 and 10. A slope range of 0 to 2% includes 34.72% of the study area, and its



265 rating (slope range = 0–2%) is 10. A rank of 9 is dedicated for 65.28% of the aquifer, which has  
266 a 2 to 6% slope (parts of the northwest) as shown in Figure 4(A) and Tables 2 and 6. As the  
267 gradient increases, the runoff increases as well (Israil et al., 2006) leading to less penetration  
268 (Jaiswal et al., 2003). Based on Madrucci et al.'s study (2008), the gradients higher than 35° are  
269 considered restrictions on groundwater desirability because of the lack of springs.

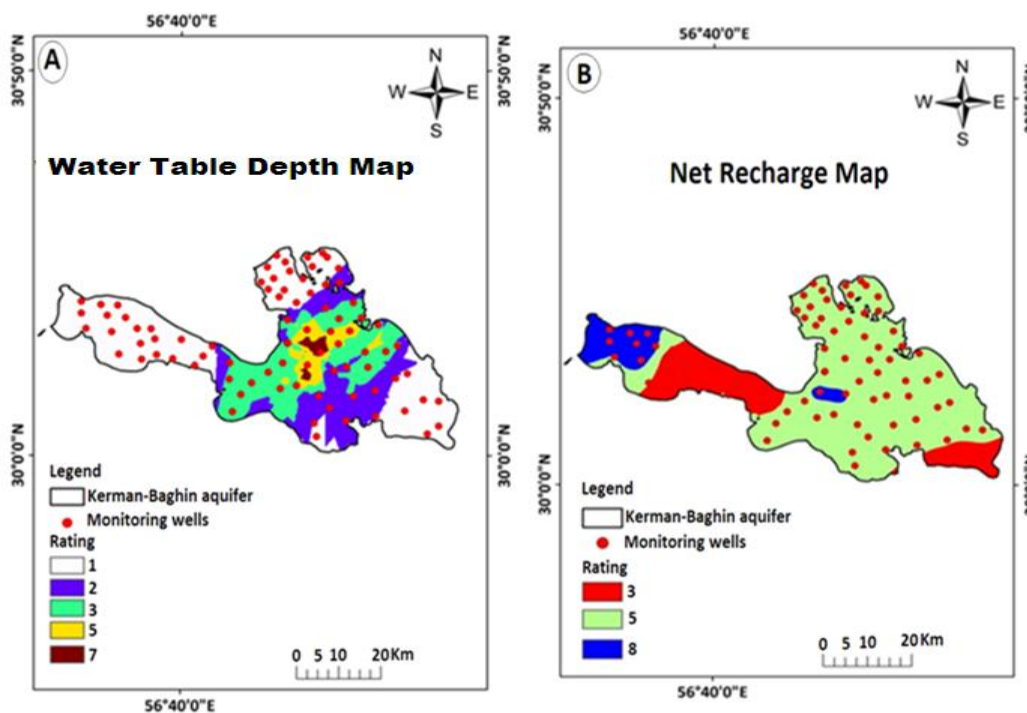
270 The Kerman–Baghin aquifer rated map of the impact of the vadose zone parameter is  
271 indicated in Figure 4(B). According to the results, the soil with a rank of 5 (gravel, sand, clay,  
272 and silt) is more effective on aquifer vulnerability (35.47%). Other various types of soils such as  
273 sand, clay, and silt (parts of the north, northeast, south, and southeast), gravel and sand (parts of  
274 the center and northwest), and rubble, sand, clay, and silt (parts of the northwest) cover 34.24%,  
275 20.39%, and 9.9% of the aquifer, respectively, as shown in Figure 4(B) and Table 6. Sandy soil  
276 is effective on groundwater occurrence because of the high rate of penetration (Srivastava and  
277 Bhattacharya, 2006). However, clay soil is arranged poorly because of the low infiltration  
278 (Manap et al., 2014b).

279 The Kerman–Baghin aquifer rated map of the hydraulic conductivity parameter is presented  
280 in Figure 5(A). The hydraulic conductivity factor shows high variability. Our study results show  
281 that the hydraulic conductivity parameter of the Kerman–Baghin aquifer varied from 0 to 81.5  
282 m/day. The potential for groundwater contamination is more for zones with high hydraulic  
283 conductivity (38.27%). As shown in Figure 5(A) and Table 6, 29.51%, 23.93%, 5.98%, and  
284 2.31% of the study areas have hydraulic conductivity in the ranges of 0 to 4.1 m/day, 12.2 to  
285 28.5 m/day, 28.5 to 40.7 m/day, and 40.7 to 81.5 m/day, respectively.

286 The Kerman–Baghin aquifer rated map of the land use parameter is presented in Figure 5(B).  
287 Our results show that the majority of the Kerman–Baghin aquifer is covered with irrigated field



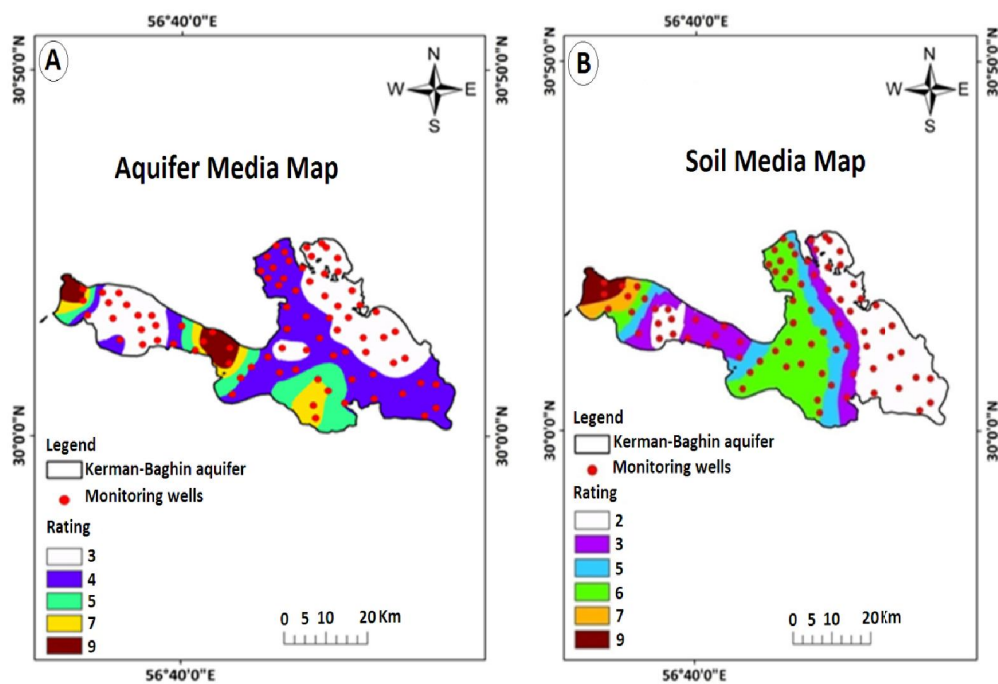
288 crops and grassland with moderate vegetation cover (20.45%). Less than 4% of land use of the  
289 study area is irrigated field crops and urban areas (3.61%), and 58.47% of land use of the study  
290 area is irrigated field crops with urban areas, grassland with poor and moderate vegetation cover,  
291 fallow land, woodland, and rocky ground. In addition, 10.17% of land use of the study area is  
292 fallow land with poor grassland and moderate vegetation cover, and 13.72% of land use of the  
293 study area is sand dunes with poor grassland and moderate vegetation cover and woodland as  
294 shown in Figure 5(B) and Tables 3 and 6.



295

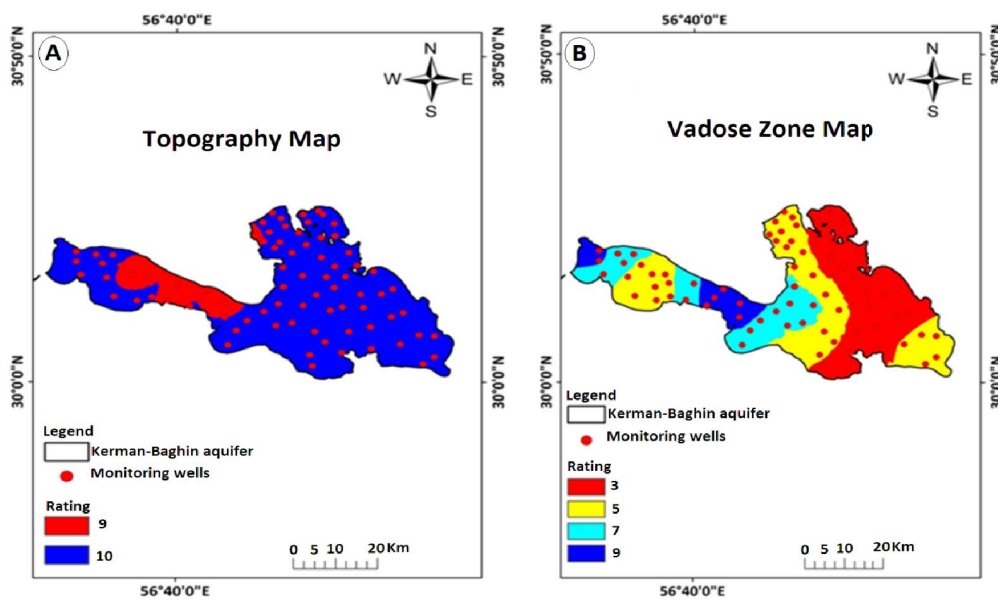
296 **Fig. 2.** Kerman–Baghin aquifer rated maps of A) water table depth and B) net recharge





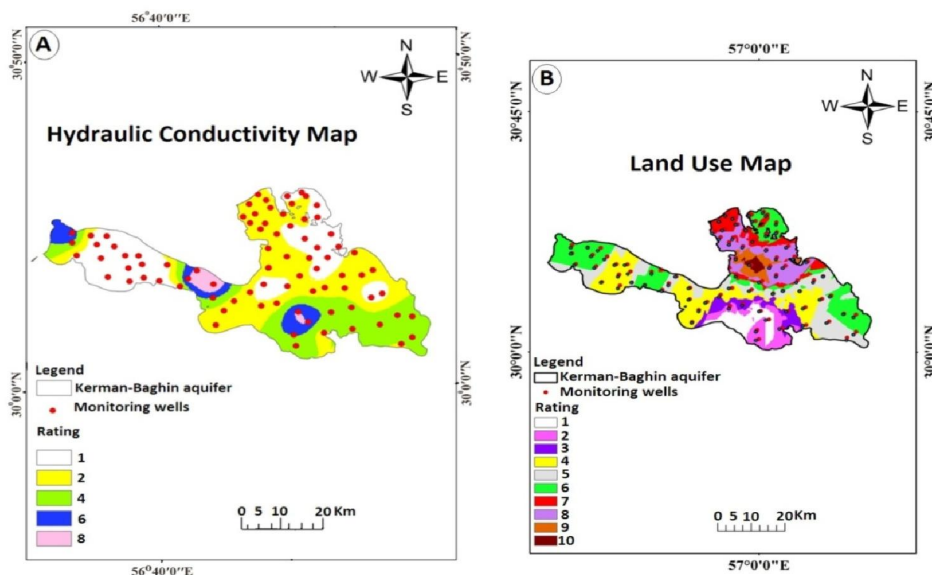
297

298 **Fig. 3.** Kerman–Baghin aquifer rated maps of A) aquifer media and B) soil media



299

300 **Fig. 4.** Kerman–Baghin aquifer rated maps of A) topography and B) vadose zone



301

302 **Fig. 5.** Kerman–Baghin aquifer rated maps of A) hydraulic conductivity and B) land use

303 **Table 6** The area of rating (km<sup>2</sup> and %) of the DRASTIC and CDRASTIC parameters

DRASTIC and CDRASTIC indexes parameters	Rating	Area (km <sup>2</sup> )	Area (%)	The aquifer geographic directions covered by the respective rating in the parameters rated maps
<b>Water table depth</b>	1	557.73	27.55	Parts of the north, south, northwest, and southeast
	2	472.18	23.34	Parts of the north south, and center
	3	469.78	23.29	Parts of the center
	5	395.00	19.53	Parts of the center
	7	129.14	6.39	Parts of the center
<b>Net recharge</b>	3	252.04	12.45	Parts of southeast, and northwest
	5	1534.15	75.81	North, northeast, south, southwest, and parts of the northwest, center, southeast
	8	237.6	11.74	Parts of the northwest and center
<b>Aquifer media</b>	3	743.18	36.72	Parts of the north, northwest, northeast, and center
	4	779.01	38.49	Parts of the north, northwest, southeast, and center
	5	207.81	10.26	Parts of the south, and northwest
	7	181.02	8.95	Parts of the south, and northwest
	9	112.76	5.58	Parts of the northwest
<b>Soil media</b>	2	658.5	32.53	Parts of the north, northwest, northeast, and southeast
	3	399.72	19.75	Parts of the north, northwest, south, and center



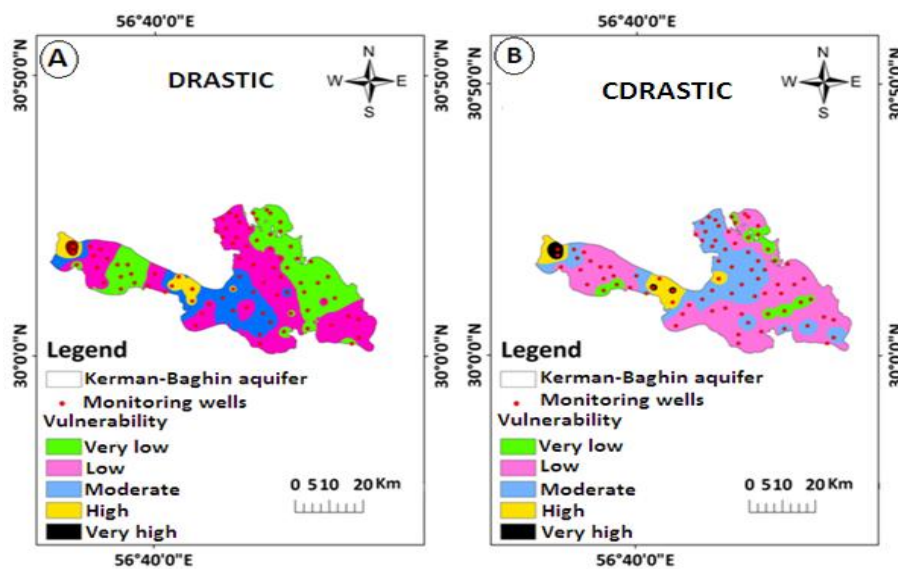
	5	297.44	14.69	Parts of the north, northwest, south, and center
	6	538.77	26.62	Parts of the northwest, center, and southwest
	7	67.56	3.33	Parts of the northwest
	9	61.79	3.08	Parts of the northwest
<b>Topography</b>	9	702.74	34.72	North, northwest, northeast, south, southeast, southwest, and center
	10	1321.07	65.28	parts of the northwest
<b>The impact of the vadose zone</b>	3	692.87	34.24	Parts of the north, northeast, south, and southeast
	5	717.91	35.47	Parts of the north, northwest, south, southeast, and center
	7	412.49	20.39	Parts of the center, and northwest
	9	200.53	9.9	Parts of the northwest
<b>Hydraulic conductivity</b>	1	597.11	29.51	Parts of the northeast, northwest, southeast, and center
	2	774.52	38.27	parts of the northwest, south, southeast and center
	4	484.17	23.93	Parts of the northwest, south, and southeast
	6	120.99	5.98	Parts of the south, and northwest
	8	46.7	2.31	Parts of the south, and northwest
<b>Land use</b>	1	112.48	5.56	Parts of the south
	2	165.02	8.16	Parts of the south
	3	205.65	10.17	Parts of the south, and center
	4	357.06	17.64	Parts of the south, southwest, northwest and center
	5	234.86	11.61	Parts of the southeast, northwest, and center
	6	413.86	20.45	Parts of the southeast, northwest, northeast, and center
	7	182.63	9.02	Parts of the north, northwest, and northeast
	8	169.4	8.37	Parts of the north, northwest, and northeast
	9	109.42	5.41	Parts of the north, northwest, and northeast
	10	73.09	3.61	Parts of the north

### 304 **3.2. DRASTIC and CDRASTIC vulnerability indexes**

305 The Kerman–Baghin aquifer vulnerability map using DRASTIC and CDRASTIC indexes is  
 306 shown in Figure 6. In the studied aquifer, the vulnerability falls under very high, high, moderate,  
 307 very low, and low vulnerable areas. It is found that in both indexes, the parts of north, northeast,  
 308 northwest, south, southwest, southeast and center come under low and very low vulnerability.  
 309 This can be attributed to low water depth, hydraulic conductivity, and net recharge in these



310 aquifer areas and the other reason might be that the aquifer media mostly are clay, sand and silt  
311 soils. The area of the vulnerability identified by investigated indexes is illustrated in Table 7.  
312 Low and very low vulnerable zones cover 25.21% and 38.31% of the Kerman–Baghin aquifer  
313 using the DRASTIC index, respectively. Very low and low vulnerable zones cover 24.95% and  
314 40.41% of the Kerman–Baghin aquifer using the CDRASTIC index, respectively. This is  
315 primarily due to water depth and relatively low permeability of the vadose zone in such aquifers  
316 (Colins et al., 2016). Around 26 % of the studied aquifer area has moderate groundwater  
317 pollution potential using DRASTIC and CDRASTIC indexes. This does not mean that such areas  
318 are without pollution but it is relatively prone to pollution when compared with other areas  
319 (Colins et al., 2016). From the DRASTIC index values, it was noticed that 10.4% of the study  
320 aquifer is under high (8.46%) and very high (1.94%) of vulnerability. The results of the study  
321 showed that 8.75% of the aquifer is under high (6.28%) and very high (2.47%) of vulnerability in  
322 the CDRASTIC index. The vulnerability maps according to these two indexes indicated very  
323 same findings, showing the northwest portion of the aquifer as the high and very high vulnerable  
324 zones. The high vulnerability can be attributed to high water depth, hydraulic conductivity, and  
325 net recharge in these aquifer areas. In addition, this can due to the high slope in this area.



326

327 **Fig. 6.** The vulnerability maps of the Kerman–Baghin aquifer by DRASTIC and CDRASTIC

328 indexes

329 **Table 7** The area of vulnerability (km<sup>2</sup> and %) identified by DRASTIC and CDRASTIC indexes

330 The sensibility of the DRASTIC index

Vulnerability	DRASTIC				composite DRASTIC			
	Ranges	Area (km <sup>2</sup> )	Area (%)	The aquifer geographic directions covered by the respective vulnerability	Ranges	Area (km <sup>2</sup> )	Area (%)	The aquifer geographic directions covered by the respective vulnerability
Very low	23-46	510.25	25.21	Parts of the south, north, northwest, and northeast	<100	505.02	24.95	Parts of the southeast, north, northwest, and northeast
Low	47-92	775.14	38.31	Parts of the south, southwest, southeast, north, northwest, northeast, and center	100-145	817.70	40.41	Parts of the south, southwest, southeast, north, northwest, northeast, and center
Moderate	93-136	527.85	26.08	Parts of the south, southwest, northwest, and center	145-190	524.06	25.89	Parts of the south, southwest, southwest, northwest, and center
High	137-184	171.02	8.46	Parts of the northwest	190-235	126.91	6.28	Parts of the northwest and center
Very high	>185	39.23	1.94	Parts of the northwest	≥235	49.79	2.47	Parts of the northwest

331

332 **3.3. Sensitivity of the DRASTIC model**



333 The MRSA to the DRASTIC index is performed by eliminating one layer data at a time as  
334 indicated in Table 8. The results showed a high variation in vulnerability index when the impact  
335 of the vadose zone factor was removed, so that, the average variation index is 1.88%. This shows  
336 that this factor is more effective in vulnerability assessment using the DRASTIC index. When  
337 this parameter is removed from the overlay process, this leads to a significant decrease in  
338 vulnerability index. This could be due to the high theoretical weight allocated to this factor  
339 (weight = 5). These findings are similar to those obtained by Dibi et al. (2012) who have shown  
340 that in addition to this parameter, topography, net recharge, and water table depth have a high  
341 impact on the vulnerability index. Also, in Samake et al. (2011) study, the impact of the vadose  
342 zone and the hydraulic conductivity parameters had a considerable impact on the vulnerability  
343 index. The vulnerability index appears to have a moderate sensitivity to the deletion of water  
344 table depth (1.48%), net recharge (1.36%), and hydraulic conductivity (1.25%) parameters. The  
345 minimum menu variation index was achieved after eliminating the aquifer media factor (0.44%),  
346 as indicated in Table 8.

347 For the estimate of the effect of individual factors towards aquifer vulnerability, the SPSA is  
348 performed. The results summary of SPSA to the DRASTIC index is shown in Table 9. The  
349 SPSA compares the effective weights and theoretical weights. The average value of the effective  
350 weight of the net recharge factor is 43.26% and its theoretical weight (%) is 17.4%. This shows  
351 that this factor is more effective in vulnerability assessment using the DRASTIC index. The  
352 results reported by other studies (Babiker et al., 2005; Doumouya et al., 2012) are similar to those  
353 of the present study. The impact of the vadose zone and water table depth parameters has high  
354 theoretical weights (21.74%). They have been dedicated with an effective weight with average  
355 value such as 8.33% and 25.55%. The remaining factors show an average value of the effective



356 weights of 14.91% (aquifer media), 9.89% (soil media), 11.35% (topography), and 7.01%  
 357 (hydraulic conductivity). The theoretical weights allocated to the water table depth, net recharge,  
 358 topography, and hydraulic conductivity parameters are not in agreement with the effective  
 359 weight. The highest and lowest impact on aquifer vulnerability was related to the net recharge  
 360 and hydraulic conductivity parameters, respectively (Table 9).

361 **Table 8** Statistical results of MRSA in the DRASTIC index

SD	Sensitivity of variability index (S) (%)			Removed parameters
	Min.	Max.	Ave.	
0.414	0.05	2.36	1.36	D
0.775	0.07	3.06	1.48	R
0.311	0.05	1.31	0.44	A
0.486	0.00	1.65	0.73	S
0.339	0.03	1.31	0.51	T
0.894	0.25	3.84	1.88	I
0.550	0.03	1.98	1.25	C

362

363 **Table 9** Statistical results of SPSA in the DRASTIC index

SD	Effective weight (%)			Theoretical weight (%)	Theoretical weight	Parameters
	Min.	Max.	Ave.			
6.179	3.23	28.46	8.33	21.74	5	D
11.998	14.06	73.47	43.26	17.4	4	R
3.190	7.26	22.13	14.91	13.04	3	A
2.916	4.49	14.29	9.89	8.7	2	S
2.222	6.45	14.71	11.35	4.3	1	T
5.367	15.79	37.31	25.55	21.74	5	I
3.738	2.42	18.75	7.01	13.04	3	C

364

### 365 3.4. The sensibility of the CDRASTIC index

366 The MRSA to the CDRASTIC index is performed by eliminating on data layer at a time as  
 367 indicated in Table 10. The mean variation index of hydraulic conductivity parameter is 4.13%.  
 368 The hydraulic conductivity has a greater effect in the aquifer vulnerability followed by water  
 369 table depth (4.05%), soil media (3.82%), topography (3.68%), aquifer media (3.28%), net  
 370 recharge (2.72%), the impact of the vadose zone (2.33%), and land use parameter (1.99%).



371 The effective weight derived from the SPSA to the CDRASTIC index is shown in Table 11.  
 372 The average value of the effective weight of the net recharge factor is 32.62%. This shows that  
 373 this factor is more effective in vulnerability assessment using CDRASTIC index. The hydraulic  
 374 conductivity displays the lowest effective weights (5.32%). The topography, net recharge, and  
 375 land use had upper effective weights toward the theoretical weights specified by CDRASTIC  
 376 index. The average value of the effective weight of the land use parameter is 24.82%. This shows  
 377 that this parameter is the second effective parameter in aquifer vulnerability using the  
 378 CDRASTIC index (Table 11).

379 **Table 10** Statistical results of MRSA in the CDRASTIC index

SD	Sensitivity of variability index (S) (%)			Removed parameters
	Min.	Max.	Ave.	
1.403	0.50	6.48	4.05	D
1.617	0.11	10.91	2.72	R
1.541	0.06	5.99	3.28	A
1.508	0.67	6.60	3.82	S
1.353	0.87	5.87	3.68	T
1.439	0.06	5.12	2.33	I
1.480	0.55	6.72	4.13	C
0.375	1.23	3.00	1.99	L

380

381 **Table 11** Statistical results of SPSA in the CDRASTIC index

SD	Effective weight (%)			Theoretical weight (%)	Theoretical weight	Parameters
	Min.	Max.	Ave.			
4.849	2.63	26.88	6.27	21.74	5	D
10.672	10.4	66.67	32.62	17.4	4	R
3.026	6.29	20.00	11.23	13.04	3	A
2.621	3.31	12.96	7.5	8.7	2	S
1.609	5.2	12.82	8.45	4.3	1	T
4.648	10.87	32.05	19.2	21.74	5	I
3.134	2.1	14.88	5.32	13.04	3	C
10.122	3.88	42.37	24.82	17.85	5	L

382

383 **4. Conclusions**





384 Evaluations of vulnerability indexes for the Kerman–Baghin aquifer were conducted using the  
385 GIS-based DRASTIC and CDRASTIC indexes. Seven hydro–geological factors (the letters  
386 comprising the acronym) are applied to determine vulnerability with DRASTIC. Eight hydro–  
387 geological parameters (one additional to the seven in DRASTIC) are utilized to determine  
388 vulnerability with the CDRASTIC index. From the DRASTIC index values, it was determined  
389 that 10.4% of the aquifer is under high (8.46%) and very high (1.94%) vulnerability. From the  
390 CDRASTIC index values, it was determined that 8.75% of the aquifer is under high (6.28%) and  
391 very high (2.47%) vulnerability. Also, we found that parts of the north, south, southeast, and  
392 northwest are under low and very low vulnerability using the DRASTIC and CDRASTIC  
393 indexes. Agricultural and industrial activities are found to be a major threat in the zones with  
394 high and very high vulnerability. The MRSA signifies the fact that hydraulic conductivity and  
395 the impact of the vadose zone factors induce a high risk of aquifer contamination according to  
396 the DRASTIC and CDRASTIC indexes, respectively. In both indexes, the SPSA analysis shows  
397 the net recharge factor as a high risk for aquifer contamination. These results indicate that the  
398 studied indexes are effective tools for determining groundwater vulnerability. Also, these results  
399 could be utilized by private and government agencies as a guide for groundwater contamination  
400 assessment in Iran.

#### 401 **Acknowledgments**

402 The authors would like to thank the Environmental Health Engineering Research Center,  
403 Kerman University of Medical Sciences, for their scientific support.

404 **Competing interests.** The authors declare that they have no conflict of interest.

#### 405 **References**



- 406 Aller, L., Truman, b., Jay H, L., Rebecca J, P., and Glen, H.: DRASTIC: a standardized system  
407 for evaluating ground water pollution potential using hydrogeologic settings, U.S Environmental  
408 Protection Agency, USA, 1985.
- 409 Ayazi, M. H., Pirasteh, S., Arvin, A., Pradhan, B., Nikouravan, B., and Mansor, S.: Disasters and  
410 risk reduction in groundwater: Zagros Mountain Southwest Iran using geoinformatics  
411 techniques, *Disaster Adv.*, 3, 51-57, 2010.
- 412 Baalousha, H.: Vulnerability assessment for the Gaza Strip, Palestine using DRASTIC, *J.*  
413 *Environ. Geol.*, 50, 405-414, <https://doi.org/10.1007/s00254-006-0219-z>, 2006.
- 414 Babiker, I. S., Mohamed, M. A., Hiyama, T., and Kato, K.: A GIS-based DRASTIC model for  
415 assessing aquifer vulnerability in Kakamigahara Heights, Gifu Prefecture, central Japan, *Sci*  
416 *Total Environ.*, 345, 127-140, <https://doi.org/10.1016/j.scitotenv.2004.11.005>, 2005.
- 417 Baghapour, M. A., Talebbeydokhti, N., Tabatabae, H., and Nobandegani, A. F.: Assessment of  
418 groundwater nitrate pollution and determination of groundwater protection zones using  
419 DRASTIC and composite DRASTIC (CD) models: the case of Shiraz unconfined aquifer, *J.*  
420 *Health. Sci. Surveill. Syst.*, 2, 54-65, 2014.
- 421 Baghapour, M. A., Nobandegani, A. F., Talebbeydokhti, N., Bagherzadeh, S., Nadiri, A. A.,  
422 Gharekhani, M., and Chitsazan, N.: Optimization of DRASTIC method by artificial neural  
423 network, nitrate vulnerability index, and composite DRASTIC models to assess groundwater  
424 vulnerability for unconfined aquifer of Shiraz Plain, Iran, *J Environ Health Sci Eng.*, 14, 1-16,  
425 <https://doi.org/10.1186/s40201-016-0254-y>, 2016.
- 426 Barber, C., Bates, L. E., Barron, R., and Allison, H.: Assessment of the relative vulnerability of  
427 groundwater to pollution: a review and background paper for the conference workshop on  
428 vulnerability assessment, *AGSO J Aust Geol Geophys.*, 14, 147-154, 1993.



- 429 Boughriba, M., Barkaoui, A.-e., Zarhloule, Y., Lahmer, Z., El Houadi, B., and Verdoya, M.:  
430 Groundwater vulnerability and risk mapping of the Angad transboundary aquifer using  
431 DRASTIC index method in GIS environment, Arab J Geosci., 3, 207-220,  
432 <https://doi.org/10.1007/s12517-009-0072-y>, 2010.
- 433 Chitsazan, M., and Akhtari, Y.: Evaluating the potential of groundwater pollution in Kherran and  
434 Zoweircherry plains through GIS-based DRASTIC model, J. Water. Wastewater, 17, 39-51,  
435 2006.
- 436 Chitsazan, M., and Akhtari, Y.: A GIS-based DRASTIC model for assessing aquifer  
437 vulnerability in Kherran Plain, Khuzestan, Iran, Water Resour Manag., 23, 1137-1155,  
438 <https://doi.org/10.1007/s11269-008-9319-8>, 2009.
- 439 Colins, J., Sashikkumar, M., Anas, P., and Kirubakaran, M.: GIS-based assessment of aquifer  
440 vulnerability using DRASTIC Model: A case study on Kodaganar basin, Earth Sci. Res. J., 20, 1-  
441 8, <https://doi.org/10.15446/esrj.v20n1.52469>, 2016.
- 442 Daly, D., and Drew, D.: Irish methodologies for karst aquifer protection, in: Beek B (ed)  
443 Hydrogeology and engineering geology of sinkholes and karst, Balkema, Rotterdam, 267-272,  
444 1999.
- 445 Dibi, B., Kouame, K. I., Konan-Waidhet, A. B., Savane, I., Biemi, J., Nedeff, V., and Lazar, G.:  
446 Impact of agriculture on the quality of groundwater resources in peri-urban zone of Songon  
447 (Cote D'ivoire), Environ. Engine. Manage. J., 11, 2173-2182,  
448 <https://doi.org/10.30638/eemj.2012.271>, 2012.
- 449 Dixon, B.: Prediction of ground water vulnerability using an integrated GIS-based Neuro-Fuzzy  
450 techniques, J. Spat. Hydro., 4, 1-38, 2004.



- 451 Doumouya, I., Dibi, B., Kouame, K. I., Saley, B., Jourda, J. P., Savane, I., and Biemi, J.:  
452 Modelling of favourable zones for the establishment of water points by geographical information  
453 system (GIS) and multicriteria analysis (MCA) in the Aboisso area (South-east of Côte d'Ivoire),  
454 Environ. Earth. Sci., 67, 1763-1780, <https://doi.org/10.1007/s12665-012-1622-2>, 2012.
- 455 Ghazavi, R., and Ebrahimi, Z.: Assessing groundwater vulnerability to contamination in an arid  
456 environment using DRASTIC and GOD models, Int. J. Environ. Sci. Tech, 12, 2909-2918,  
457 <https://doi.org/10.1007/s13762-015-0813-2>, 2015.
- 458 Ghosh, T., and Kanchan, R.: Aquifer vulnerability assessment in the Bengal alluvial tract, India,  
459 using GIS based DRASTIC model, Model Earth Syst Environ., 2, 2-13,  
460 <https://doi.org/10.1007/s40808-016-0208-5>, 2016.
- 461 Israil, M., Al-hadithi, M., Singhal, D., Kumar, B., Rao, M. S., and Verma, S.: Groundwater  
462 resources evaluation in the Piedmont zone of Himalaya, India, using Isotope and GIS techniques,  
463 J. Spatial. Hydro., 6, 107-119, 2006.
- 464 Jaiswal, R., Mukherjee, S., Krishnamurthy, J., and Saxena, R.: Role of remote sensing and GIS  
465 techniques for generation of groundwater prospect zones towards rural development--an  
466 approach, Int J Remote Sens., 24, 993-1008, <https://doi.org/10.1080/01431160210144543>, 2003.
- 467 Jaseela, C., Prabhakar, K., and Harikumar, P. S. P.: Application of GIS and DRASTIC modeling  
468 for evaluation of groundwater vulnerability near a solid waste disposal site, Int. J. Geosci., 7,  
469 558-571, <https://doi.org/10.4236/ijg.2016.74043>, 2016.
- 470 Javadi, S., Kavehkar, N., Mousavizadeh, M., and Mohammadi, K.: Modification of DRASTIC  
471 model to map groundwater vulnerability to pollution using nitrate measurements in agricultural  
472 areas, J. Agr. Sci. Tech., 13, 239-249, 2010.



- 473 Javadi, S., Kavehkar, N., Mohammadi, K., Khodadadi, A., and Kahawita, R.: Calibrating  
474 DRASTIC using field measurements, sensitivity analysis and statistical methods to assess  
475 groundwater vulnerability, *Water. Int.*, 36, 719-732,  
476 <https://doi.org/10.1080/02508060.2011.610921>, 2011.
- 477 Jayasekera, D., Kaluarachchi, J. J., and Villholth, K. G.: Groundwater Quality Impacts Due to  
478 Population Growth and Land Use Exploitation in the Coastal Aquifers of Sri Lanka, Southern  
479 Illinois University Carbondale 2008, 43,
- 480 Jayasekera, D. L., Kaluarachchi, J. J., and Villholth, K. G.: Groundwater stress and vulnerability  
481 in rural coastal aquifers under competing demands: a case study from Sri Lanka, *Environ Monit*  
482 *Assess.*, 176, 13-30, <https://doi.org/10.1007/s10661-010-1563-8>, 2011.
- 483 Kardan Moghaddam, H., Jafari, F., and Javadi, S.: Vulnerability evaluation of a coastal aquifer  
484 via GALDIT model and comparison with DRASTIC index using quality parameters, *Hydro. Sci.*  
485 *J.*, 62, 137-146, <https://doi.org/10.1080/02626667.2015.1080827>, 2017.
- 486 Kumar, P., Thakur, P. K., Bansod, B. K., and Debnath, S. K.: Assessment of the effectiveness of  
487 DRASTIC in predicting the vulnerability of groundwater to contamination: a case study from  
488 Fatehgarh Sahib district in Punjab, India, *Environ. Earth. Sci.*, 75, 879,  
489 <https://doi.org/10.1007/s12665-016-5712-4>, 2016.
- 490 Madrucci, V., Taioli, F., and de Araújo, C. C.: Groundwater favorability map using GIS  
491 multicriteria data analysis on crystalline terrain, Sao Paulo State, Brazil, *J. Hydro.*, 357, 153-173,  
492 <https://doi.org/10.1016/j.jhydrol.2008.03.026>, 2008.
- 493 Manap, M. A., Sulaiman, W. N. A., Ramli, M. F., Pradhan, B., and Surip, N.: A knowledge-  
494 driven GIS modeling technique for groundwater potential mapping at the Upper Langat Basin,  
495 Malaysia, *Arabian. J. Geosci.*, 6, 1621-1637, <https://doi.org/10.1007/s12517-011-0469-2>, 2013.



- 496 Manap, M. A., Nampak, H., Pradhan, B., Lee, S., Sulaiman, W. N. A., and Ramli, M. F.:  
497 Application of probabilistic-based frequency ratio model in groundwater potential mapping using  
498 remote sensing data and GIS, *Arabian. J.Geosci.*, 7, 711-724, [https://doi.org/10.1007/s12517-](https://doi.org/10.1007/s12517-012-0795-z)  
499 012-0795-z, 2014a.
- 500 Manap, M. A., Nampak, H., Pradhan, B., Lee, S., Sulaiman, W. N. A., and Ramli, M. F.:  
501 Application of probabilistic-based frequency ratio model in groundwater potential mapping using  
502 remote sensing data and GIS, *Arabian. J. Geosci.*, 7, 711-724, [https://doi.org/10.1007/s12517-](https://doi.org/10.1007/s12517-012-0795-z)  
503 012-0795-z, 2014b.
- 504 Martínez-Bastida, J. J., Arauzo, M., and Valladolid, M.: Intrinsic and specific vulnerability of  
505 groundwater in central Spain: the risk of nitrate pollution, *Hydro. J.*, 18, 681-698,  
506 <https://doi.org/10.1007/s10040-009-0549-5>, 2010.
- 507 Merchant, J. W.: GIS-based groundwater pollution hazard assessment: a critical review of the  
508 DRASTIC model, *Photogramm Eng Remote Sensing.*, 60, 1117-1127, 1994.
- 509 Modabberi, H., Hashemi, M. M. R., Ashournia, M., and Rahimpour, M. A.: Sensitivity Analysis  
510 and Vulnerability Mapping of the Guilan Aquifer Using Drastic Method, *Rev. Environ. Earth.*  
511 *Sci.*, 4, 27-41, <https://doi.org/10.18488/journal.80.2017.41.27.41>, 2017.
- 512 Napolitano, P., and Fabbri, A.: Single-parameter sensitivity analysis for aquifer vulnerability  
513 assessment using DRASTIC and SINTACS, *Proceedings of the Vienna Conference*,  
514 Netherlands, 1996, 559-566,
- 515 Neshat, A., Pradhan, B., Pirasteh, S., and Shafri, H. Z. M.: Estimating groundwater vulnerability  
516 to pollution using a modified DRASTIC model in the Kerman agricultural area, Iran, *Environ.*  
517 *Earth. Sci.*, 71, 3119-3131, <https://doi.org/10.1007/s12665-013-2690-7>, 2014.



- 518 Neshat, A., and Pradhan, B.: Evaluation of groundwater vulnerability to pollution using  
519 DRASTIC framework and GIS, *Arabian. J. Geosci.*, 10, 2-8, [https://doi.org/10.1007/s12517-017-](https://doi.org/10.1007/s12517-017-3292-6)  
520 3292-6, 2017.
- 521 Raju, N. J., Ram, P., and Gossel, W.: Evaluation of groundwater vulnerability in the lower  
522 Varuna catchment area, Uttar Pradesh, India using AVI concept, *J. Geol. Soc. India.*, 83, 273-  
523 278, <https://doi.org/10.1007/s12594-014-0039-9>, 2014.
- 524 Saida, S., Tarik, H., Abdellah, A., Farid, H., and Hakim, B.: Assessment of groundwater  
525 vulnerability to nitrate based on the optimised DRASTIC models in the GIS Environment (Case  
526 of Sidi Rached Basin, Algeria), *Geosciences*, 7, 2-23,  
527 <https://doi.org/10.3390/geosciences7020020>, 2017.
- 528 Saidi, S., Bouri, S., and Ben Dhia, H.: Sensitivity analysis in groundwater vulnerability  
529 assessment based on GIS in the Mahdia-Ksour Essaf aquifer, Tunisia: a validation study, *Hydro.*  
530 *Sci. J.*, 56, 288-304, <https://doi.org/10.1080/02626667.2011.552886>, 2011.
- 531 Samake, M., Tang, Z., Hlaing, W., Mbue, I. N., Kasereka, K., and Balogun, W. O.: Groundwater  
532 vulnerability assessment in shallow aquifer in Linfen Basin, Shanxi Province, China using  
533 DRASTIC model, *J. Sustain. Develop.*, 4, 53-71, <https://doi.org/10.5539/jsd.v4n1p53>, 2011.
- 534 Sarah, C., and Patricia I, C.: Ground water vulnerability assessment: Predicting relative  
535 contamination potential under conditions of uncertainty, National Academies Press, USA, 1993.
- 536 Secunda, S., Collin, M., and Melloul, A. J.: Groundwater vulnerability assessment using a  
537 composite model combining DRASTIC with extensive agricultural land use in Israel's Sharon  
538 region, *J. Environ. Manage.*, 54, 39-57, <https://doi.org/10.1006/jema.1998.0221>, 1998.



539 Shirazi, S. M., Imran, H., and Akib, S.: GIS-based DRASTIC method for groundwater  
540 vulnerability assessment: a review, *J. Risk. Res.*, 15, 991-1011,  
541 <https://doi.org/10.1080/13669877.2012.686053>, 2012.

542 Singh, A., Srivastav, S., Kumar, S., and Chakrapani, G. J.: A modified-DRASTIC model  
543 (DRASTICA) for assessment of groundwater vulnerability to pollution in an urbanized  
544 environment in Lucknow, India, *Environ. Earth. Sci.*, 74, 5475-5490,  
545 <https://doi.org/10.1007/s12665-015-4558-5>, 2015.

546 Souleymane, K., and Tang, Z.: A novel method of sensitivity analysis testing by applying the  
547 DRASTIC and fuzzy optimization methods to assess groundwater vulnerability to pollution: the  
548 case of the Senegal River basin in Mali, *Nat. Hazards. Earth. Sys. Sci.*, 17, 1375-1392,  
549 <https://doi.org/10.5194/nhess-17-1375-2017>, 2017.

550 Srivastava, P. K., and Bhattacharya, A. K.: Groundwater assessment through an integrated  
551 approach using remote sensing, GIS and resistivity techniques: a case study from a hard rock  
552 terrain, *Int. J. Remote. Sens.*, 27, 4599-4620, <https://doi.org/10.1080/01431160600554983>,  
553 2006.

554 Tilahun, K., and Merkel, B. J.: Assessment of groundwater vulnerability to pollution in Dire  
555 Dawa, Ethiopia using DRASTIC, *Environ. Earth. Sci.*, 59, 1485-1496,  
556 <https://doi.org/10.1007/s12665-009-0134-1>, 2010.

557 Zghibi, A., Merzougui, A., Chenini, I., Ergaieg, K., Zouhri, L., and Tarhouni, J.: Groundwater  
558 vulnerability analysis of Tunisian coastal aquifer: an application of DRASTIC index method in  
559 GIS environment, *Groundwater. Sustain. Develop.*, 2, 169-181,  
560 <https://doi.org/10.1016/j.gsd.2016.10.001>, 2016.

561